Flexible and Transparent Dielectric Film with a High Dielectric Constant Using Chemical Vapor Deposition-Grown Graphene Interlayer

Jin-Young Kim,[†] Jongho Lee,[‡] Wi Hyoung Lee,[§] Iskandar N. Kholmanov,[†,∥] Ji Won Suk,[†,¶] TaeYoung Kim,[†] Yufeng Hao,[†] Harry Chou,[†] Deji Akinwande,[‡] and Rodney S. Ruoff[†,*]

[†]Department of Mechanical Engineering and the Materials Science and Engineering Program, The University of Texas at Austin, Austin, Texas 78712, United States, [‡]Department of Electrical and Computer Engineering, Microelectronics Research Center, The University of Texas at Austin, Austin, Texas 78758, United States, [§]Department of Organic and Nano System Engineering, Konkuk University, Seoul, 143-701 Korea, [∥]CNR-IDASC Sensor Lab, Department of Chemistry and Physics, University of Brescia, via Valotti, 9, Brescia 25133, Italy, and [¶]School of Mechanical Engineering, Sungkyunkwan University, Suwon, 440-746 Korea

ABSTRACT We have devised a dielectric film with a chemical vapor deposited graphene interlayer and studied the effect of the graphene interlayer on the dielectric performance. The highly transparent and flexible film was a polymer/graphene/polymer 'sandwich-structure' fabricated by a one-step transfer method that had a dielectric constant of 51, with a dielectric loss of 0.05 at 1 kHz. The graphene interlayer in the film forms a space charge layer, *i.e.*, an accumulation of polarized charge carriers near the graphene, resulting in an induced space charge polarization and enhanced dielectric constant. The characteristic of the space charge layer for the graphene dielectric film, the sheet resistance of the graphene interlayer, was adjusted through thermal annealing that caused partial oxidation. The dielectric film with higher sheet resistance due to the oxidized graphene interlayer had a significantly lower dielectric constant compared to that with the graphene with lower interlayer sheet resistance. Oxidizing the graphene interlayer yields a smaller and thinner space charge density in the dielectric film, ultimately leading to decreased capacitance. Considering the simplicity of the fabrication process and high dielectric performance, as well as the high transparency and flexibility, this film is promising for applications in plastic electronics.

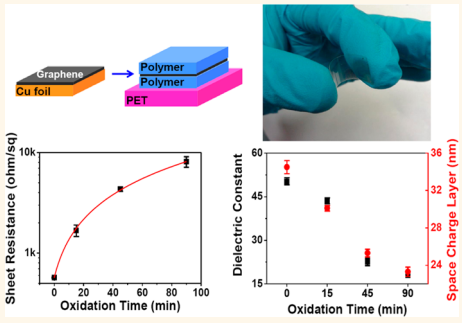

KEYWORDS: graphene · graphene transfer · polymer · space charge polarization · dielectric performance

Graphene, a monolayer of sp^2-bonded carbon atoms, has attracted interest because of its optical, electrical, and mechanical properties that also suggest it is a strong candidate for use in plastic electronics.[1−5] A common method for the synthesis of large-area and high-quality monolayer graphene is chemical vapor deposition (CVD) of hydrocarbon on copper substrates such as Cu foil.[6] Chemically modified graphene (CMG) such as reduced graphene oxide has been studied for dielectric applications. Doping CMG with halogen elements or mixing it with ferroelectric ceramics in composites can induce a high dielectric constant.[4,7,8] In these kinds of composite films, one of the important properties is the conductivity of the CMG filler, which enhances the dielectric constant since it is strongly related to the capacitance.[4,9] CVD-grown graphene may give even further enhanced dielectric properties because the conductivity of CVD-grown graphene is higher than that of CMG. One strategy is to use the CVD-grown graphene as an interlayer between the polymer layers. The CVD-grown graphene would induce space charge polarization at the interface between the graphene and polymer, resulting in increased capacitance.

Here, we introduce a new type of transparent and flexible dielectric film using a CVD-grown graphene interlayer and we study the role of the graphene interlayer in the film. This dielectric film had a polymer/graphene/polymer sandwich-structure that was fabricated by a simple one-step transfer method onto a polymer-coated

* Address correspondence to r.ruoff@mail.utexas.edu.

Received for review July 19, 2013 and accepted December 4, 2013.

Published online 10.1021/nn406058g

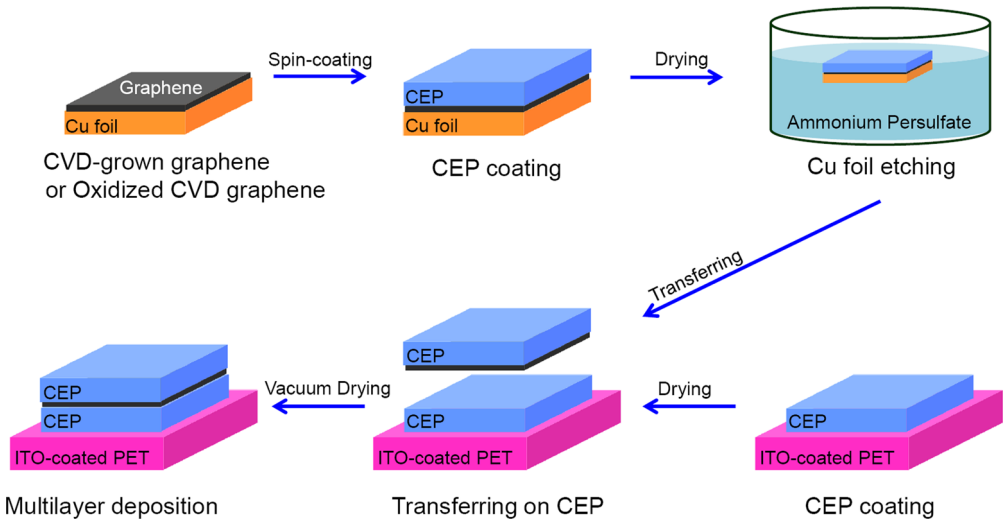

Figure 1. Fabrication of the graphene dielectric film by a one-step transfer method. Either pristine graphene or oxidized graphene was used as an interlayer in the film.

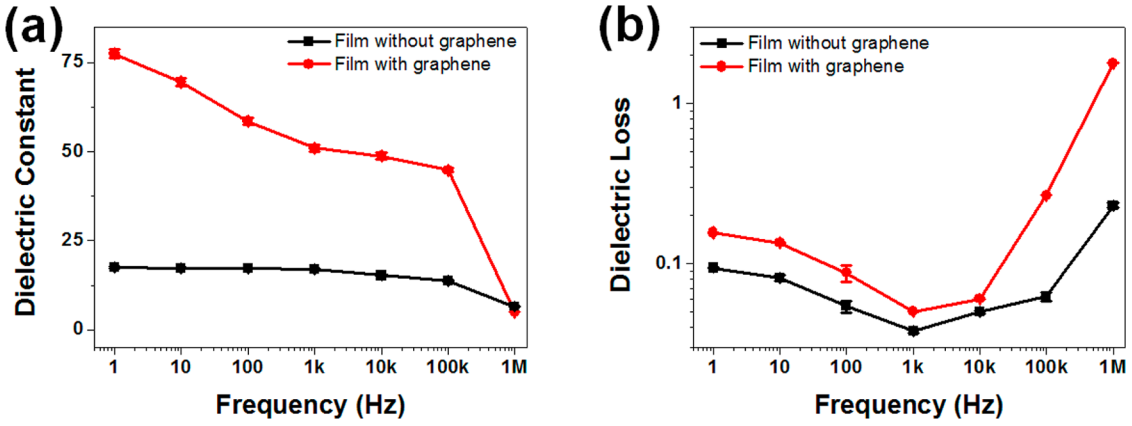

Figure 2. (a) The dielectric constant and (b) dielectric loss (*i.e.*, dielectric loss tangent) of the dielectric film with and without the graphene interlayer as a function of applied frequencies ranging from 1 Hz to 1 MHz.

polyethylene terephthalate (PET) substrate. These films showed dramatically enhanced dielectric performance with high transparency and flexibility. The mechanism for enhancing the dielectric constant was investigated by Raman spectroscopy and electrical characterization.

RESULTS AND DISCUSSION

Figure 1 shows the fabrication process of the polymer/graphene/polymer sandwich-structured dielectric film (hereafter referred to as a graphene dielectric film) by a one-step transfer method. This method is a simple and easy fabrication process to produce the graphene dielectric film. The thicknesses of the upper and lower polymer films were 0.90 and 0.84 μm, respectively (for a total thickness of 1.74 μm), as shown in Figure S1. The interface between the graphene and the polymer is clearly seen in the scanning electron microscope (SEM) image (see Figure S1). The dielectric performance of the neat polymer and the graphene dielectric film was measured at an applied voltage of 0.1 V and frequencies in the range of 1 Hz to 1 MHz. Both films showed a decreased (increased) dielectric constant (dielectric loss) with increasing frequency due to relaxation (see Figure 2a,b).[10−12] The dielectric constant of the graphene dielectric film was 77 with a dielectric loss of 0.156, while that of the neat polymer was 17 with a dielectric loss of 0.094 at 1 Hz. At a frequency of 1 kHz, the dielectric constant of the graphene dielectric film was 51 with a dielectric loss of 0.05, while that of the neat polymer was 17 with a dielectric loss of 0.038. The capacitance density of the film with and without graphene was also calculated, as shown in Figure S2. The capacitance densities of the film with and without graphene interlayer were 25.9 and 8.6 nF/cm^2, respectively, at 1 kHz. The graphene dielectric film showed a 3-fold increase in the dielectric constant with a low dielectric loss compared to the neat polymer film at 1 kHz. At low frequencies of 1 Hz to 10 kHz, the graphene dielectric film gives a high dielectric constant which decreases rapidly compared to the neat polymer. This behavior can be explained by the space charge polarization phenomenon.[13−15] This phenomenon

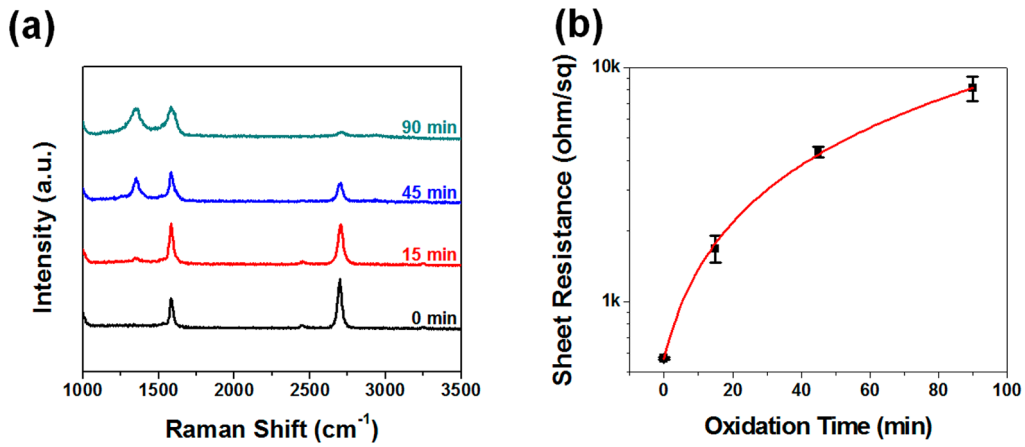

Figure 3. (a) Raman spectra of the CVD-grown graphene films before and after the thermal annealing treatment for 0, 15, 45, and 90 min in air. (b) Sheet resistance *versus* oxidation time of the graphene film on SiO_2/Si substrates before and after the thermal annealing treatment for 0, 15, 45, and 90 min.

results in a large enhancement in the dielectric constant of the graphene dielectric film. As has been shown for the conductive filler and polymer composite system, the graphene interlayer polarizes to be n type while the polymer turns predominately p type.[16,17] At the interface between the graphene and the polymer, negative charges accumulate on the surface of the graphene while positive charges accumulate in the polymer region near the graphene to maintain electroneutrality,[18−21] as shown in Figure S3. The increment in the local electric field near graphene may promote charge accumulation. These charge accumulation processes can induce the formation of a space charge layer, resulting in enhanced capacitance.[18−21] The dielectric strength was also measured for the neat polymer and the graphene dielectric film, as shown in Figure S4. In the polymer film, the avalanche mechanism is known to be a factor for the dielectric breakdown. When an external electric field is applied to the polymer film, free electrons in the polymer are accelerated along the mean free path and gain a higher energy which initiates the breakdown.[22,23] The leakage current density of the graphene dielectric film was 1×10^{-3} A/cm^2 at an electric field of 10 V/μm, while that of the neat polymer was low, giving 9.87×10^{-7} A/cm^2 at the same electric field. For the case of the graphene dielectric film, the graphene interlayer enhances the local electric field and increases the electron tunneling even at a relatively low electric field. This decreases the dielectric strength of the graphene dielectric film.

To investigate the space charge effect from the graphene interlayer, the sheet resistance was controllably varied. Thermal annealing for 0 (*i.e.*, pristine graphene), 15, 45, and 90 min in air yielded oxidized graphene with different sheet resistance values. Figure 3a shows Raman spectra of the oxidized graphene films. The intensity of the D-band, which is a defect-related peak corresponding to the presence of point defects, residual oxygen, and structural disorder,[24,25] increased with increasing oxidation time. Meanwhile, the 2D-band (in-plane optical vibrations) decreased, as shown in Figure S5. The position of the 2D-band was blue-shifted after thermal annealing, as shown in Figure S6. The shift is due to the oxygen or oxygen-containing functional group bonding with the graphene basal plane and/or edges during the thermal annealing, forming the sp^3-bonds.[26−28] To measure the sheet resistance of the oxidized graphene films, the graphene films were transferred onto SiO_2/Si substrates. Figure 3b shows the electrical properties of the graphene films. The sheet resistances of the oxidized graphene (for 0, 15, 45, and 90 min) were 570, 1680, 4340, and 8140 Ω/sq, respectively. These results demonstrate that the electrical conductivity of the oxidized graphene decreased with increasing oxidation time of the graphene interlayer.

Graphene dielectric films were also made using the oxidized graphene interlayer. Figure 4a,b shows the dielectric performance at 0.1 V and 1 kHz. The dielectric constants of the graphene dielectric films for 0, 15, 45, and 90 min (thermal annealing times) were 50, 44, 23, and 18, respectively. The dielectric losses of all films were less than 0.053. The dielectric constant dramatically decreased with increasing thermal annealing time. This behavior can be explained by the different charges that accumulated at the interface between the graphene and the polymer, which led to the formation of the space charge layer.[18,29,30] When the graphene film was treated by thermal annealing, the electron carrier density decreased in the oxidized graphene due to the p-doping. This strongly affected the space charge properties by decreasing the space charge density and layer thickness in the graphene dielectric film, leading to decreased capacitance.[18] Figure S7 shows the relationship between the sheet resistance of the graphene interlayer and the dielectric constant of the graphene dielectric film in oxidized graphene

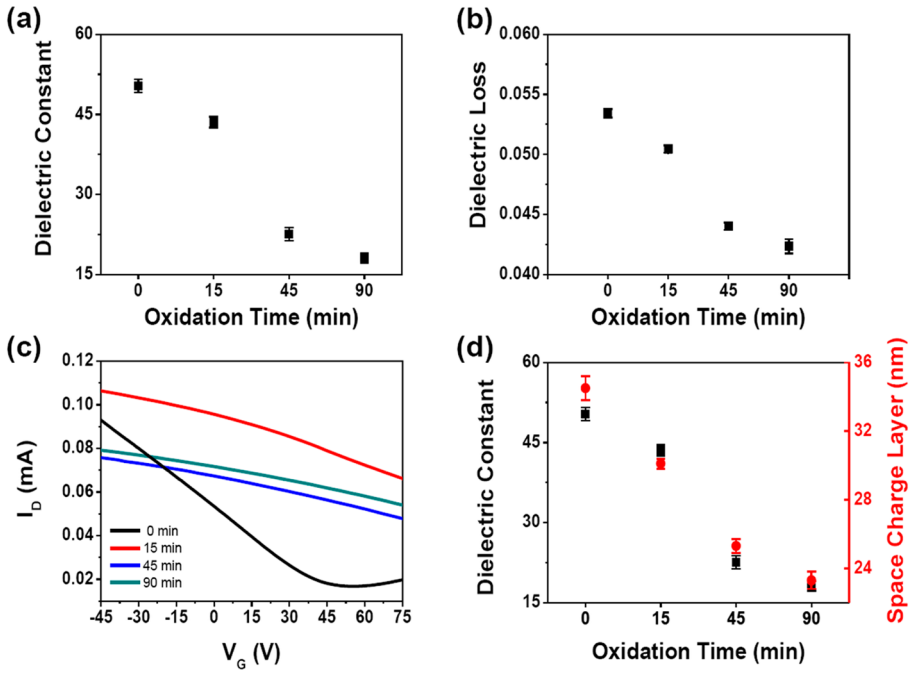

Figure 4. (a) Dielectric constant and (b) dielectric loss (*i.e.*, dielectric loss tangent) of the graphene dielectric films with the graphene interlayer before and after the thermal annealing treatment for 0, 15, 45, and 90 min at 1 kHz. (c) Current−voltage (I_D−V_G) curves for the GFETs measured in air using the graphene obtained before and after thermal annealing for times of 0, 15, 45, and 90 min. (d) The dielectric constant of the graphene dielectric films at 1 kHz and the calculated thickness of the space charge layer as a function of the graphene interlayer before and after the thermal annealing treatment for 0, 15, 45, and 90 min.

films. The dielectric constant of the graphene dielectric film decreased with increasing sheet resistance. This result supports the presence and characteristics of a space charge layer. In addition, to evaluate the thickness of the space charge layer of the graphene dielectric film, back-gated graphene field-effect transistors (GFETs) were made using a 285 nm-thick SiO_2 layer as the gate dielectric. All of the GFETs using partially oxidized CVD-grown graphene as the interlayer exhibit no detectable V_{Dirac} even when the gate voltage was swept to 80 V due to the significant p-doping of the graphene (see Figure 4c). The hole mobility can be obtained by using the following equation:[31]

$$\mu = \frac{1}{C_i}\frac{d\sigma}{dV_G} \quad (1)$$

where $C_i = 1.1 \times 10^{-8}$ F cm^{-2}. The hole mobility of oxidized graphenes for 0, 15, 45, and 90 min of oxidation was 2645, 1400, 757, and 601 cm^2/(V·s), respectively. The space charge layer thickness of the graphene dielectric film using the oxidized graphene as the interlayer was calculated with[30]

$$W_p = \sqrt{\frac{2\varepsilon\varepsilon_0 U_S}{e^2 N_D}} \quad (2)$$

where ε is the dielectric constant of the graphene dielectric film, ε_0 is the dielectric constant of vacuum, U_S is a potential barrier height, e is the elementary charge, and N_D is a doping density. The space charge layer thicknesses of the graphene interlayer for 0, 15, 45, and 90 min of oxidation were 35 ± 0.7, 30 ± 0.3, 25 ± 0.4, and 23 ± 0.5 nm, respectively, assuming U_S: 2.0 eV.[32] Figure 4d shows the relationship between the dielectric constant and the thickness of the space charge layer of the graphene dielectric film with the oxidized graphene films. The dielectric constant of the graphene dielectric film decreased with decreasing thickness of the space charge layer. This result supports the presence and characteristics of a space charge layer. Figure S8 shows the voltage dependence of the dielectric constant for the neat polymer and graphene dielectric films at 1 kHz. This has a parabolic shape. This trend is due to the polarization saturation in the higher voltage region.[33] The maximum dielectric constant is often located at zero voltage; however, it could shift toward negative bias (from −1.0 to −1.5 V) due to the presence of some positive charges.[33] The maximum dielectric constants of our films were located at around −1.0 V.

Large-area graphene dielectric films with high dielectric constant were successfully fabricated on PET substrates, and the high transparency and flexibility of the films are shown in Figure 5a. To better quantify the transparency and flexibility, optical transmittance measurements and bending tests were performed as shown in Figure 5b,c. In the visible range of 390−760 nm, the optical transmittance of the graphene dielectric film was higher than 88%. The optical transmittance at a wavelength of 550 nm was 93%. Figure 5c

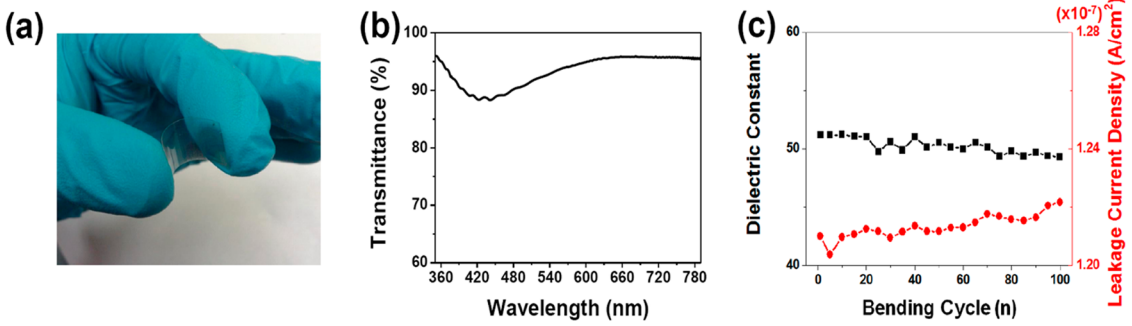

Figure 5. (a) Digital camera image of the graphene dielectric film on a PET substrate. This dielectric film has high transparency and flexibility. (b) Optical transmittance of the graphene dielectric film as a function of the wavelength ranging from 350 to 790 nm. (c) The dielectric constant and the leakage current density of the graphene dielectric films as a function of bending, up to 100 times.

shows the dielectric constant and the leakage current density of the graphene dielectric film as a function of the number of cycles bending (up to 100) times, at a 7.5 mm bending radius. The initial value of the dielectric constant (the leakage current density at 0.1 V) was 51.2 (1.210×10^{-7} A/cm^2). After 100 cycles of bending, the graphene dielectric film exhibited a 3.4% (1.1%) decrease (increase) in dielectric constant (leakage current density) compared to the initial value. This indicates that the graphene dielectric film has good adhesion between each of the component layers and high tensile strength. This graphene dielectric film, which has a high dielectric constant, is highly transparent, and highly flexible, might be a strong candidate for plastic electronic applications. In addition, the thin layer (1.74 μm) is likely to be beneficial for applications of plastic electronics compared to other types of composite films (see Table S9).

CONCLUSIONS

We have successfully fabricated a transparent and flexible dielectric film with a high dielectric constant using a CVD-grown graphene interlayer and studied the role of the graphene interlayer in this film. The graphene dielectric film consisted of a polymer/graphene/polymer structure on a PET substrate which was made by a one-step transfer method. The resulting graphene dielectric films had a dielectric constant of 51, with a dielectric loss of 0.05 at 1 kHz. The space charge layer resulting from the different charge accumulation (*i.e.*, space charge polarization) near the graphene interlayer in the film enhanced the dielectric constant.

EXPERIMENTAL SECTION

Graphene Synthesis and Device Fabrication. Figure 1 shows the fabrication process of the graphene dielectric film. First, large-area monolayer graphene films containing 2−10% multilayer regions were synthesized by a low pressure CVD process.[6] A 25-μm-thick copper foil (Alfa Aesar, 13382) was loaded into a tube furnace and heated to 1035 °C. After annealing with 2 sccm of H_2 for 10 min, 5 sccm of CH_4 is then introduced to synthesize the graphene (total pressure of ~80 mTorr). Twelve weight pervent cyanoethyl pullulan polymer (CEP) dissolved in 82 wt % *N*,*N*-dimethylformamide (DMF) was spin-coated onto the as-grown graphene film on copper foil. The films were then flattened by pressing them between two cover glass slides, and the structure was then dried at 130 °C for 30 min. The CEP-coated graphene film was floated in a 0.1 M ammonium persulfate ($(NH_4)_2S_2O_8$) solution to etch the copper. After all of the copper had been etched away, the CEP-coated graphene films were transferred to another CEP (dried at 130 °C for 30 min)-coated glass or PET substrate, then dried in vacuum. Cr(5 nm)−Au(50 nm) electrodes were then deposited onto the films by thermal evaporation. The total thickness of the graphene dielectric film was under 1.74 μm. For the case of the oxidized CVD-grown graphene, the graphene/copper foil was placed on a hot-plate at 250 °C for 15, 45, or 90 min in ambient air. To investigate the performance of graphene field-effect transistors (GFETs), back-gated GFETs were made using 285-nm SiO_2/Si wafer by a method similar to that reported in our previous paper.[5]

Characterization. The GFETs performance of oxidized graphenes and the dielectric properties of the graphene dielectric films on ITO-coated glass or PET were measured with a semiconductor device analyzer (Agilent, B1500A). The thicknesses of the graphene dielectric films were obtained with a Detak 6 M Stylus Surface Profilometer. The optical transmittance of the graphene dielectric film was examined by spectroscopic ellipsometry (J.A. Wollam, M2000). To characterize the oxidized graphene, the oxidized graphene films were transferred onto SiO_2/Si substrates with the aid of PMMA (996 K). After the removal of PMMA, the oxidized graphene films were then characterized by Raman (WiTec Alpha (488 nm laser wavelength) analysis and electrical tests.

Conflict of Interest: The authors declare no competing financial interest.

Acknowledgment. We appreciate support from the Office of Naval Research.

Supporting Information Available: SEM of the graphene dielectric film; capacitance densities of the dielectric film *vs* applied frequencies; schematic diagram of the mechanism for enhancing the capacitance; leakage current density *vs* applied field; intensity of the D- and 2D-bands of the graphene films and position of the 2D-band *vs* thermal annealing; dielectric constant of the graphene dielectric films *vs* sheet resistance of the graphene interlayer; tabular comparison of some dielectric properties for various composite materials. This material is available free of charge *via* the Internet at http://pubs.acs.org.

REFERENCES AND NOTES

1. Zhu, Y. W.; Murali, S.; Cai, W. W.; Li, X. S.; Suk, J. W.; Potts, J. R.; Ruoff, R. S. Graphene and Graphene Oxide: Synthesis,

Properties, and Applications. *Adv. Mater.* **2010**, *22*, 3906–3924.
2. Stankovich, S.; Dikin, D. A.; Dommett, G. H. B.; Kohlhaas, K. M.; Zimney, E. J.; Stach, E. A.; Piner, R. D.; Nguyen, S. T.; Ruoff, R. S. Graphene-Based Composite Materials. *Nature* **2006**, *442*, 282–286.
3. Dreyer, D. R.; Ruoff, R. S.; Bielawski, C. W. From Conception to Realization: An Historial Account of Graphene and Some Perspectives for Its Future. *Angew. Chem., Int. Ed.* **2010**, *49*, 9336–9344.
4. Kim, J. Y.; Lee, W. H.; Suk, J. W.; Potts, J. R.; Chou, H.; Kholmanov, I. N.; Piner, R. D.; Lee, J.; Akinwande, D.; Ruoff, R. S. Chlorination of Reduced Graphene Oxide Enhances the Dielectric Constant of Reduced Graphene Oxide/Polymer Composites. *Adv. Mater.* **2013**, *25*, 2308–2313.
5. Lee, W. H.; Suk, J. W.; Lee, J.; Hao, Y. F.; Park, J.; Yang, J. W.; Ha, H. W.; Murali, S.; Chou, H.; Akinwande, D.; *et al.* Simultaneous Transfer and Doping of CVD-Grown Graphene by Fluoropolymer for Transparent Conductive Films on Plastic. *Acs Nano* **2012**, *6*, 1284–1290.
6. Li, X. S.; Cai, W. W.; An, J. H.; Kim, S.; Nah, J.; Yang, D. X.; Piner, R.; Velamakanni, A.; Jung, I.; Tutuc, E.; *et al.* Large-Area Synthesis of High-Quality and Uniform Graphene Films on Copper Foils. *Science* **2009**, *324*, 1312–1314.
7. Wang, Z. P.; Nelson, J. K.; Hillborg, H.; Zhao, S.; Schadler, L. S. Graphene Oxide Filled Nanocomposite with Novel Electrical and Dielectric Properties. *Adv. Mater.* **2012**, *24*, 3134–3137.
8. Wang, Z. P.; Nelson, J. K.; Miao, J. J.; Linhardt, R. J.; Schadler, L. S.; Hillborg, H.; Zhao, S. Effect of High Aspect Ratio Filler on Dielectric Properties of Polymer Composites: A Study on Barium Titanate Fibers and Graphene Platelets. *IEEE Trans. Dielectr. Electr. Insul.* **2012**, *19*, 960–967.
9. Dang, Z. M.; Zhang, Y. H.; Tjong, S. C. Dependence of Dielectric Behavior on the Physical Property of Fillers in the Polymer-Matrix Composites. *Synth. Met.* **2004**, *146*, 79–84.
10. Chen, C. Y.; Birgeneau, R. J.; Kastner, M. A.; Preyer, N. W.; Thio, T. Frequency and Magnetic-Field Dependence of the Dielectric-Constant and Conductivity of La_2CuO_{4+y}. *Phys. Rev. B* **1991**, *43*, 392–401.
11. Bertram, B. D.; Gerhardt, R. A.; Schultz, J. W. Impedance Response and Modeling of Composites Containing Aligned Semiconductor Whiskers: Effects of dc-Bias Partitioning and Percolated-Cluster Length, Topology, and Filler Interfaces. *J. Appl. Phys.* **2012**, *111*, 124913/1–124913/14.
12. Bertram, B. D.; Gerhardt, R. A. Effects of Frequency, Percolation, and Axisymmetric Microstructure on the Electrical Response of Hot-Pressed Alumina-Silicon Carbide Whisker Composites. *J. Am. Ceram. Soc.* **2011**, *94*, 1125–1132.
13. Murugaraj, P.; Mainwaring, D.; Mora-Huertas, N. Dielectric Enhancement in Polymer-Nanoparticle Composites through Interphase Polarizability. *J. Appl. Phys.* **2005**, *98*, 054302/1–054304/6.
14. Jiang, M. J.; Dang, Z. M.; Bozlar, M.; Miomandre, F.; Bai, J. B. Broad-Frequency Dielectric Behaviors in Multiwalled Carbon Nanotube/Rubber Nanocomposites. *J. Appl. Phys.* **2009**, *106*, 084902/1–084902/6.
15. Nan, C. W.; Shen, Y.; Ma, J. Physical Properties of Composites Near Percolation. *Annu. Rev. Mater. Res.* **2010**, *40*, 131–151.
16. Coleman, J. N.; Curran, S.; Dalton, A. B.; Davey, A. P.; McCarthy, B.; Blau, W.; Barklie, R. C. Percolation-Dominated Conductivity in a Conjugated-Polymer-Carbon-Nanotube Composite. *Phys. Rev. B* **1998**, *58*, R7492–R7495.
17. Curran, S. A.; Ajayan, P. M.; Blau, W. J.; Carroll, D. L.; Coleman, J. N.; Dalton, A. B.; Davey, A. P.; Drury, A.; McCarthy, B.; Maier, S.; *et al.* A Composite from Poly(m-phenylenevinylene-co-2,5-dioctoxy-p-phenylenevinylene) and Carbon Nanotubes: A Novel Material for Molecular Optoelectronics. *Adv. Mater.* **1998**, *10*, 1091–1093.
18. Wang, B. H.; Liang, G. Z.; Jiao, Y. C.; Gu, A. J.; Liu, L. M.; Yuan, L.; Zhang, W. Two-Layer Materials of Polyethylene and a Carbon Nanotube/Cyanate Ester Composite with High Dielectric Constant and Extremely Low Dielectric Loss. *Carbon* **2013**, *54*, 224–233.
19. Tang, Z. C. W.; Sun, L. L.; Li, B.; Zhong, W. H. Structurally Induced Dielectric Constant Promotion and Loss Suppression for Poly(vinylidene fluoride) Nanocomposites. *Macromol. Mater. Eng.* **2012**, *297*, 420–426.
20. Sun, L. L.; Li, B.; Zhao, Y.; Mitchell, G.; Zhong, W. H. Structure-Induced High Dielectric Constant and Low Loss of CNF/PVDF Composites with Heterogeneous CNF Distribution. *Nanotechnology* **2010**, *21*, 305702/1–305702/8.
21. Xu, X. B.; Li, Z. M.; Shi, L.; Bian, X. C.; Xiang, Z. D. Ultralight Conductive Carbon-Nanotube-Polymer Composite. *Small* **2007**, *3*, 408–411.
22. Artbauer, J. Electric Strength of Polymers. *J. Phys. D: Appl. Phys.* **1996**, *29*, 446–456.
23. Barber, P.; Balasubramanian, S.; Anguchamy, Y.; Gong, S.; Wibowo, A.; Gao, H.; Ploehn, H. J.; zur Loye, H. C. Polymer Composite and Nanocomposite Dielectric Materials for Pulse Power Energy Storage. *Materials* **2009**, *2*, 1697–1733.
24. Eda, G.; Fanchini, G.; Chhowalla, M. Large-Area Ultrathin Films of Reduced Graphene Oxide as a Transparent and Flexible Electronic Material. *Nat. Nanotechnol.* **2008**, *3*, 270–274.
25. Schniepp, H. C.; Li, J. L.; McAllister, M. J.; Sai, H.; Herrera-Alonso, M.; Adamson, D. H.; Prud'homme, R. K.; Car, R.; Saville, D. A.; Aksay, I. A. Functionalized Single Graphene Sheets Derived from Splitting Graphite Oxide. *J. Phys. Chem. B* **2006**, *110*, 8535–8539.
26. Ryu, S.; Liu, L.; Berciaud, S.; Yu, Y. J.; Liu, H. T.; Kim, P.; Flynn, G. W.; Brus, L. E. Atmospheric Oxygen Binding and Hole Doping in Deformed Graphene on a SiO_2 Substrate. *Nano Lett.* **2010**, *10*, 4944–4951.
27. Zhou, H. Q.; Qiu, C. Y.; Yu, F.; Yang, H. C.; Chen, M. J.; Hu, L. J.; Guo, Y. J.; Sun, L. F. Raman Scattering of Monolayer Graphene: The Temperature and Oxygen Doping Effects. *J. Phys. D: Appl. Phys.* **2011**, *44*, 185404/1–185404/6.
28. Pantelic, R. S.; Suk, J. W.; Hao, Y. F.; Ruoff, R. S.; Stahlberg, H. Oxidative Doping Renders Graphene Hydrophilic, Facilitating Its Use as a Support in Biological TEM. *Nano Lett.* **2011**, *11*, 4319–4323.
29. Chen, Q.; Du, P. Y.; Jin, L.; Weng, W. J.; Han, G. R. Percolative Conductor/Polymer Composite Films with Significant Dielectric Properties. *Appl. Phys. Lett.* **2007**, *91*, 022912/1–022912/3.
30. Nersesyan, S. R.; Petrosyan, S. G. Depletion Length and Space Charge Layer Capacitance in Doped Semiconductor Nanoshpere. *Semicond. Sci. Technol.* **2012**, *27*, 125009/1–125009/4.
31. Schwierz, F. Graphene Transistors. *Nat. Nanotechnol.* **2010**, *5*, 487–496.
32. Rahman, R.; Servati, P. Effects of Inter-Tube Distance and Alignment on Tunnelling Resistance and Strain Sensitivity of Nanotube/Polymer Composite Films. *Nanotechnology* **2012**, *23*, 055703/1–055703/9.
33. Quan, Z.; Zhang, B. S.; Zhang, T. J.; Zhao, X. Z.; Pan, R. K.; Ma, Z. J.; Jiang, J. Interfacial Characteristics and Dielectric Properties of $Ba_{0.65}Sr_{0.35}TiO_3$ Thin Films. *Thin Solid Films* **2008**, *516*, 999–1005.